Proton Driver Front End
Focusing Solenoid Quench Protection Studies.
Part I: Method Description and the First Iteration

I. Terechkine, P. Bauer

This note describes quench protection studies made in preparation for testing focusing solenoids of the Front End of the Proton Driver (PD).

Quench events are inevitable during the testing, and configuration of the testing setup must ensure safety of the solenoid, power supply, and other test equipment during this event. Protection of the solenoid is usually reached by switching off the power supply and by quick removal of the energy stored in the magnetic field. Whether this energy evacuation is possible or not can be found only after knowing details of quench propagation in the solenoid. To make this analysis, one must answer the next questions:

1. How fast does quench propagate from the start point to other parts of the coil?
2. What temperature of the normal parts of the coil can be after the quench?
3. What can be resistance of the coil?
4. How the current in the coil behaves after the power supply is made off?
5. What voltage in the coil can we expect?
6. What voltage can be detected in the early stage of the quench using voltage taps?
7. Can we use this voltage to control the test stand protection system?

Answering these questions is important before engaging in the test planning activities.

This study is devoted to a specific issue of the quench dynamics in the Test Solenoid, being built to work on fabrication issues. The results of the study are not universal, but used techniques can be applied to analyze other solenoids. As a tool for this study MathCad spreadsheets were used. More efforts are required to come out with a software that would automate some of the steps made manually in this study and provide more options for a designer. These kinds of efforts, although quite attractive, are not included in our nearest action plan.

I. Coil layout and the main assumptions

The layout of the Test Solenoid is show in Fig. 1 below.

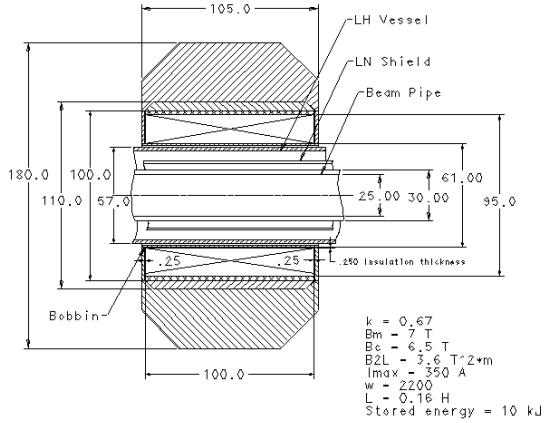

Fig. 1: Test solenoid layout

It is possible to see that the solenoid is relatively short and clearly does not have uniform magnetic field within the bore of the beam pipe. Nevertheless for the purpose of getting results fast, we will accept that the magnetic filed does not change in the longitudinal direction. In the radial direction we will accept that in the winding the field changes linearly with radius, which is quite close to the reality.

One of the most important parameters of the coil is a ratio between the maximal magnetic field in the winding and the current. In our case, the value of this coefficient (for the test solenoid shown in Fig. 1) is **0.0188 T/A**. The number of turns in the coil is **2200** and the number of layers is **20**. Other relevant coil design information can be found in Fig. 1. Properties of the superconductor will be discussed later.

Although the round wire was used to wind the sample coil, in this exercise we used equivalent rectangular wire with the same number of layers: N = 20. We assume that the insulation thickness between the layers of the coil is twice as large as the insulation thickness between the turns in the same layer. Taking into the account this assumption and knowing the coil geometry, it is quite straightforward to come out with the equivalent wire dimensions and insulation thickness. Equivalent compaction factor of this winding was adjusted to have wire cross-section equal to that of the round NbTi SSC-type strand. This equivalent compaction factor k = 0.664, which is quite close to the value 0.67 achieved during the sample coil winding. The total cross-section area of bare strand is $0.513*10^{-6}$ m^2. The height of one layer (including insulation) is $0.85*10^{-3}$ m and the width of one turn is $0.91*10^{-3}$ m (including insulation). The insulation thickness between the turns in the layer is $97.4*10^{-6}$ m and between the layers the insulation is $195*10^{-6}$ m thick.

Now when we know the structure of the coil, we are ready to start the analysis of quench propagation. But first the relevant properties of all materials used to build the coil must be found and expressed in a convenient manner as functions of temperature and magnetic filed, so that we could use them in the MathCad environment.

II. Material properties

Mostly these properties were borrowed from work of P. Bauer on the analysis of quench propagation in the high field dipole, although some data have different source. Below the parameterization of each particular property will be presented accompanied by the corresponding graph. We are talking about the next set of properties:

1. Specific heat
2. Thermal conductivity
3. Specific resistance
4. Superconducting wire critical surface and critical parameters of the strand

Because the coil insulation is made of fiberglass impregnated with epoxy, properties of this insulation are close to those of G-10 material.

II-1 Specific heat

Specific heat parameterization for Cu with RRR = 50 and corresponding graph are shown below in Fig. 2. Similar data from NbTi and for epoxy-impregnated glass fibers (G-10) are shown in Fig. 3 and Fig. 4.

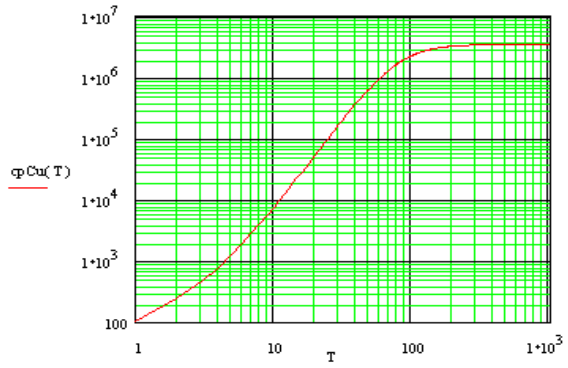

$\gamma Cu := 0.011$ J/K^2/kg $\rho Cu := 8960$ kg/m^3

$\beta Cu := 0.000744$ J/K^4/kg $cpCu300 := 3.454 \cdot 10^6$ J/K/m^3

$$cpCulow(T) := \left(\gamma Cu \cdot \rho Cu \cdot T + \beta Cu \cdot \rho Cu \cdot T^3\right)$$

$$cpCu(T) := \frac{1}{\left(\frac{1}{cpCu300}\right) + \left(\frac{1}{cpCulow(T)}\right)} \quad \text{J/K/m^3}$$

Fig. 2: Specific Heat of Copper (RRR = 50)

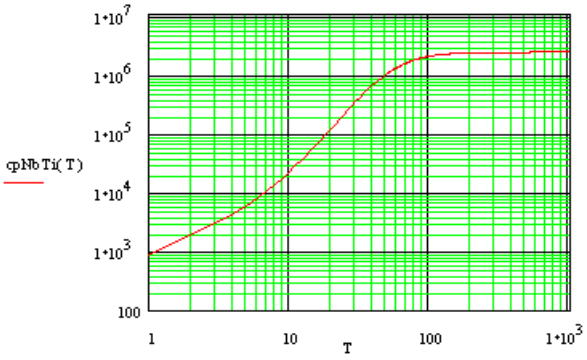

$\gamma NbTi := 0.145$ $\rho NbTi := 6000$

$\beta NbTi := 0.0023$ $cpNbTi300 := 2.304 \cdot 10^6$

$$cpNbTilow(T) := \left(\gamma NbTi \cdot \rho NbTi \cdot T + \beta NbTi \cdot \rho NbTi \cdot T^3\right)$$

$$cpNbTi(T) := \frac{1}{\left(\frac{1}{cpNbTi300}\right) + \left(\frac{1}{cpNbTilow(T)}\right)} \quad \text{J/K/m^3}$$

Fig. 3: Specific Heat of NbTi

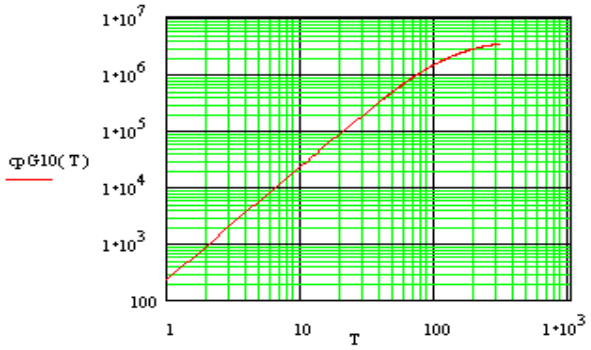

$\gamma G10 := 0$ $\rho G10 := 1900$

$\beta G10 := 0.125$ $cpG10\_300 := 4 \cdot 10^6$

$$cpG10low(T) := \left(\gamma G10 \cdot \rho G10 \cdot T + \beta G10 \cdot \rho G10 \cdot T^2\right)$$

$$cpG10(T) := \frac{1}{\left(\frac{1}{cpG10\_300}\right) + \left(\frac{1}{cpG10low(T)}\right)} \quad \text{J/K/m^3}$$

Fig. 4: Specific Heat of G-10

II-2. Thermal conductivity

Thermal conductivity dependence on temperature were found in available reference materials and tabulated with subsequent interpolation. Corresponding tables and graphs are provided below. Units for λ are W/m-K

Table 1: Thermal Conductivity of Copper (RRR = 50)

T (K)	4	6	8	10	20	30	50	70	90	110	300
λ(Cu)	500	700	950	1150	2000	1900	1050	650	500	400	390

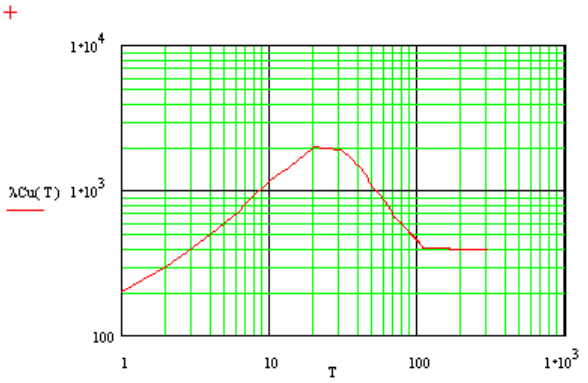

Fig. 5: Thermal conductivity of copper (RRR = 50)

Table 2: Thermal conductivity of G-10

T (K)	2	4	6	10	20	50	80	100	200	300
λ(G10)	0.03	0.057	0.082	0.12	0.17	0.24	0.3	0.32	0.45	0.65

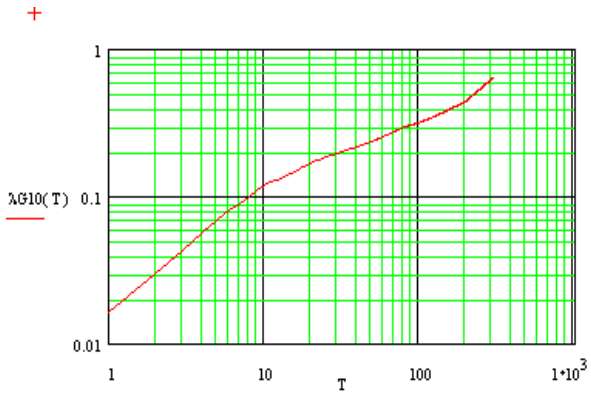

Fig. 6: Thermal conductivity of G-10

II-3. Specific Resistance

Universal expression for the specific resistance of copper that takes into the account purity (RRR) of copper and magnetic field is shown accompanied with a corresponding graph in Fig. 7 below.

$$\rho 1(T) := \frac{1.171 \cdot 10^{-17} \cdot (T)^{4.49}}{1 + \left[4.5 \cdot 10^{-7} \cdot (T)^{3.35} \cdot e^{-\left(\frac{50}{T}\right)^{6.428}} \right]}$$

$$\rho 2(T) := \left(\frac{1.69 \cdot 10^{-8}}{RRR} + \rho 1(T) + 0.4531 \cdot \frac{1.69 \cdot 10^{-8} \cdot \rho 1(T)}{RRR \cdot \rho 1(T) + 1.69 \cdot 10^{-8}} \right)$$

$$A(T,B) := \log\left(1.553 \cdot 10^{-8} \cdot \frac{B}{\rho 2(T)} \right)$$

$$a(T,B) := -2.662 + 0.3168 \cdot A(T,B) + 0.6229 \cdot A(T,B)^2 - 0.1839 \cdot A(T,B)^3 + 0.01827 \cdot A(T,B)^4$$

$$rhoCu(T,B) := \rho 2(T) \cdot \left(1 + 10^{a(T,B)} \right)$$

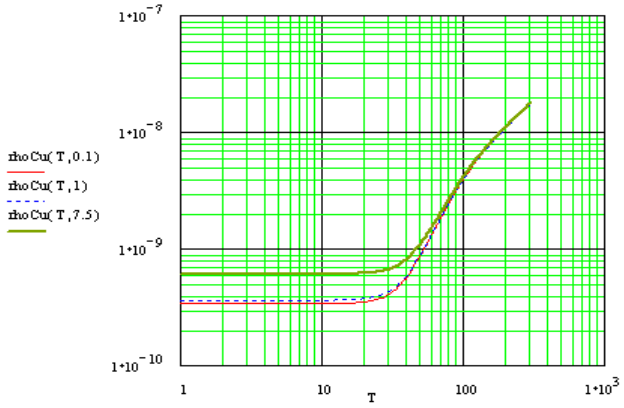

Fig. 7: Specific resistance of copper as a function of temperature.
B = 0.1 T, 1 T, and 7.5 T; RRR = 50

II-4. Critical Surface of NbTi

Parameterization of the critical surface for NbTi was made many times by many authors, including A. Devret (Fig. 8). Although quite reliable, this way of presenting the critical surface has proved to be quite time consuming when used in the MathCad environment when the spreadsheet must performed multiple calculations. Simpler (although probably less precise) expression was used (Fig. 9) that gave quite satisfactory representation of the critical surface within the required range of parameters. For both the plots, critical current density is plotted versus magnetic field with the strand temperature as a parameter.

$$Jc0 := 2500 \cdot 10^6$$

$$a1 := 0.315319 \qquad a4 := 0.163089 \qquad a7 := 0.020418$$

$$a2 := 0.01528 \qquad a5 := 0.231741$$

$$a3 := 0.00161 \qquad a6 := 0.021249$$

$$Jc(B,T) := Jc0 \cdot \left[1 - \frac{\left[a1 \cdot (T - T0) + a2 \cdot (T - T0)^2 - a3 \cdot (T - T0)^3\right]}{1 - a4 \cdot (B - 5)}\right] \cdot \frac{(1 - a5 \cdot (B - 5))}{1 - a6 \cdot (B - 5) - a7 \cdot (B - 5)^2}$$

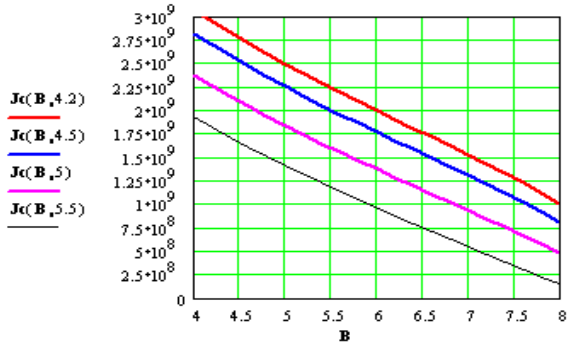

Fig. 8. Critical Surface of NbTi. Old representation

$$Jc(B,T) := 2.5\cdot10^{9}\cdot\left[\frac{(Tc0 - T)}{Tc0 - T0}\right]^{1.8} - 5.4\cdot10^{8}\cdot(B - 5) + 2.5\cdot10^{7}\cdot(B - 5)^{2} \qquad A/m^2$$

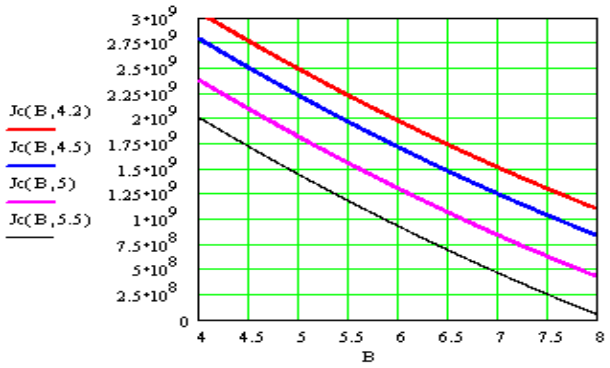

Fig. 9. Critical Surface of NbTi. New representation.

To switch from the current density to the strand current, it is necessary to know content of NbTi and copper in the strand. This content is defined by a copper-to-non-copper ratio, which is $\gamma = 1.3$ for the SSC strand that will be used in the coil. The cross-section of superconductor in the strand can be found as $A_{sc} = A_{met}/(1+\gamma)$ and copper cross-section is $A_{Cu} = A_{met}^{*} \gamma /(1+ \gamma)$. Taking this into the account, strand current (for the strand size described earlier) can be calculated knowing the current density in the superconductor:

$$I = J_{sc} * A_{met}/(1+\gamma)$$

So, critical surface of the strand can be plotted in terms of strand critical current as a series of curves with the strand temperature as a parameter (see Fig. 10).

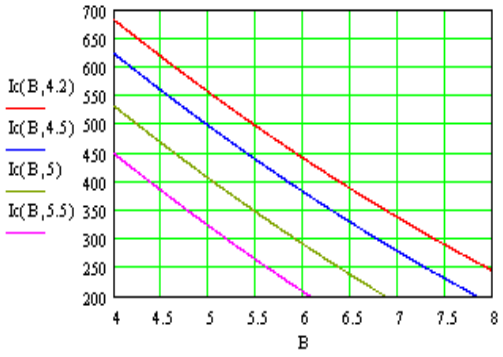

Fig. 10: Critical surface of the strand used in the coil of the solenoid.

Knowing this critical surface it is possible to calculate temperature of a particular turn of the solenoid winding (that carries the current ***I*** and is in the magnetic field ***B***) at the moment when it starts loosing its property of superconductivity. An example of how this critical temperature depends on the coil current is shown in Fig. 11 for a turn in the first layer, which is exposed to the maximal field. It is possible to see that the maximal current that the strand in the coil can carry at 4.5 K is 340 A. If to lower current, the critical temperature increases and at about 190 A it becomes quite close to the ultimate critical temperature of NbTi of 9.2 K corresponding to I = 0 and B = 0.

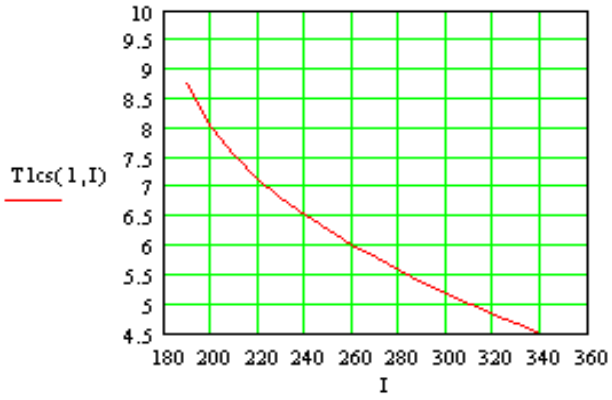

Fig. 11: Critical temperature for a turn in the first layer of the coil.

To simplify further modeling using MathCad environment, calculation of these curves of critical current for different layers were simplified by using the expression in Fig. 12, that shows a set of the critical temperature curves for turns in different layers of the coil. This expression was obtained by first finding $T_{cs}(n, I)$ using representation in Fig. 10 and then by applying parameterization in a convenient form. Definitely, other ways can be found of doing this transformation.

$$F(n,I) := \left[I + 125 \cdot \left(0.0188 \cdot \frac{Nlayers + 1 - n}{Nlayers} \cdot I - 5 \right) - 7.5 \cdot \left(0.0188 \cdot \frac{Nlayers + 1 - n}{Nlayers} \cdot I - 5 \right)^2 \right]$$

$$F1(n,I) := if(F(n,I) > 0, F(n,I), 0)$$

$$Tcs(n,I) := Tc0 - (Tc0 - T0) \cdot \left(\frac{F1(n,I)}{565} \right)^{\frac{1}{1.8}}$$

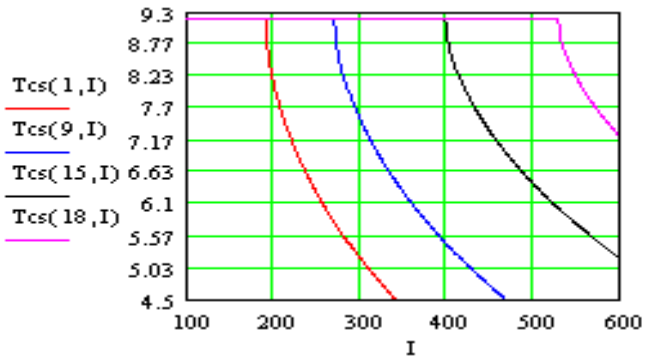

Fig. 12: Critical temperature as a function of coil current and the number of the layer.

After the preparation work described above, we can start analysis of quench propagation in the coil. Quench can start in any turn of the coil due to many reasons. Some of them are listed below:

- Magnetic flux line movement due to loss of pinning;
- Mechanical movement of a part of a turn;
- High frequency noise in the current source;
- Energy deposition due to radiation.

Underlying physical reason of transition to normal state is increase of temperature in a turn above the critical level. Because the temperature margin is lower for the first layer, it has the highest probability to quench. In the next chapter we'll try to find what is going to happen after a part of a turn in the middle of the first layer becomes normal.

III. Quench Propagation.

As was mentioned earlier, we will assume that for some reason a portion of a turn in the center of the first layer of the coil makes a transition to normal state. If this portion is large enough, the normal state starts propagating in an uncontrollable manner; in other words, coil "quenches". There are three routes for quench propagation:

1. Spiraling along the strand;
2. Propagating along the layer;
3. Propagating in the radial direction (across the layers)

III-1. Quench propagation along strands

We will start the analysis with the quench propagation along the strand. This case was studied by many authors, so we will use the expression for the rate of the quench propagation in the adiabatic case from [1]:

$$v_{strand}(n,I) = \frac{I\cdot(1+\gamma)}{S_{met}\cdot(C_{pCu}(T_{av}(n,I))\cdot\gamma + C_{pNbTi}(T_{av}(n,I)))}\cdot\left[\frac{\rho_{Cu}(T_{av}(n,I),B(n,I))\cdot\lambda_{Cu}(T_{av}(n,I))}{T_{cs}(n,I)-T_{w0}}\right]^{\frac{1}{2}}$$

In this expression, I is the coil current at the moment when the temperature of some small part of the strand reaches T_{cs} - critical temperature at this current and magnetic field B(n,I). We will use properties of material at the temperature T_{av}, which is the average between $T_{cs}(n,I)$ (at this temperature, the layer n with current I the temperature starts transition) and the temperature of the "cold" part of the winding (or bath temperature) T_{w0}. In this study we will accept T_{w0} = 4.5 K. Obviously, quench propagation velocity will depend on the layer number at given current because the critical temperature increases and the field strength drops with radius.

As we now have analytical expressions for the material properties and critical surface, it is quite straightforward to use the expression for $v_{strand}(n,I)$ to get results we are looking for. They are presented graphically in Fig. 13 in two forms: propagation velocity in meters per second as a function of the current with the layer number as a parameter and as a function of a layer number with the current as a parameter. Obviously these two forms are equivalent.

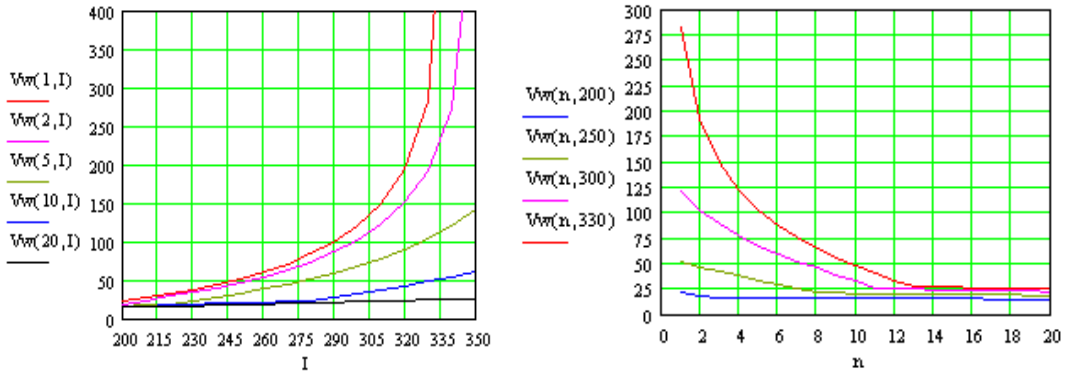

Fig. 13: Quench propagation velocity along the strand.

It is easy to see from the graphs in Fig. 13 that the propagation velocity depends strongly on the current and on the layer number (magnetic field). As one could expect, the propagation rate is higher for the inner layers (with stronger field), but for the outer layers, the dependence on the current and on the layer number is quite weak. Physical reason of this is that the critical temperature for low field is close to the ultimate critical temperature of the superconductor (that is T_c = 9.2 K, the critical temperature at I = 0, B = 0 - see Fig. 14).

$$Tc(B) := Tc0 \cdot \left[1 - \left(\frac{B}{Bc20}\right)\right]^{0.59}$$

Fig. 14: Critical temperature as a function of magnetic field at zero current.

Another important quench propagation characteristic is a delay in the normal transition from one turn to the next one due to propagation along the strand:

$$Del_{strand} = \frac{2\pi R(n)}{v_{strand}(n, I)} \qquad \text{with} \qquad R(n) = R_{in} + (R_{out} - R_{in}) \cdot \frac{n-1}{N_l}$$

Corresponding graph is presented in Fig. 15. It will be compared later with the delay of quench propagation across the layers and between turns along the axis.

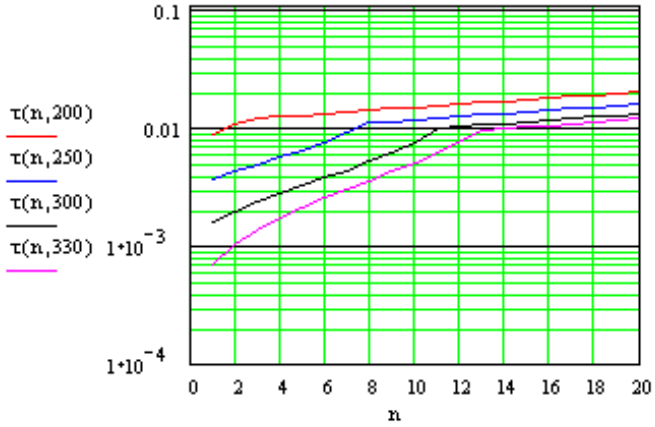

Fig. 15: Turn-to-turn quench delay time due to propagation along strand

III-2. Quench propagation in the transverse direction

As soon as temperature of any part of the coil increases, heat diffusion (thermal conductivity) will work to transfer the heat from a hot area to colder one. It is possible to evaluate the rate of this process if we know temperature of the source turn (T_{cs} at quench) and the receiving turns (initially T_{w0}), thermal conductivity of the insulation between the

layers, and specific heat values of the relevant materials. While in the normal state, the source turn will dissipate power. The amount of this power depends on the current and on the specific resistance at the temperature of the source. Thickness and width (per one turn) of the interlayer insulation was found earlier; we will use symbols ***h*** and ***w*** for these quantities. Thermal conductivities of all the materials depend on temperature; we will use the average temperature for this estimate. The temperature of the superconducting strand will increase due to the heat coming from the normal strand; the rate of this increase will be defined also by specific heat of NbTi (at its temperature). In this part we are going to find a delay time of quench propagation between the layers, that is the moment when the temperature of the receiver becomes the critical temperature at given current and magnetic field (layer number).

The system of equations that describe the process is written below in terms of finite difference problem, which can be solved by stepping. Here indexes "*i*" and "*i+1*" refer to the previous and the next states separated by a time step "*dt*". T1 and T2 are temperatures of the source and the receiving turns correspondingly.

$$T1_{i+1} = T1_i + \frac{\rho_{Cu}(T1_i, B(n,I)) \cdot (\gamma+1)^2}{\gamma \cdot (C_{pCu}(T1_i) \cdot \gamma + C_{pNbTi}(T1_i))} \cdot \left[\frac{I}{A_{met}}\right]^2 \cdot dt$$

$$\Phi_i = \lambda_{G10}\left[\frac{T1_i + T2_i}{2}\right] \cdot \frac{w}{h} \cdot (T1_i - T2_i)$$

$$T2_{i+1} = T2_i + \frac{\Phi_i}{A_{met} \cdot \left[\frac{C_{pCu}(T2_i) \cdot \gamma}{\gamma - 1} + \frac{C_{pNbTi}(T2_i)}{\gamma - 1} + \frac{C_{pG10}(T2_i) \cdot (1-k)}{k}\right]} \cdot dt$$

The first equation defines temperature rise of the source during one time step due to resistive heating. The heating power is much higher then the heat transfer, so the adiabatic condition is well justified. The second equation defines heat transfer. The third equation describes temperature rise in NbTi to transferred heat. It takes into the account also the temperature rise of the insulation between the layers (and partially on the sides).

By solving these equations, a series of graphs was produced that allowed extracting information about the moment when the receiver's temperature reaches its critical value. Fig. 16a shows the temperature rise for the layer n = 9, that quenches at the moment t = 0 (curve T1) and for the layer n = 10 (curve T2). Temperature of this layer is reaching the critical temperature for the current 300 A and the magnetic field for the 10-th layer (which is ~ 8.1 K) at the moment t = 0.0026 s, as shows the graph in Fig. 16b.

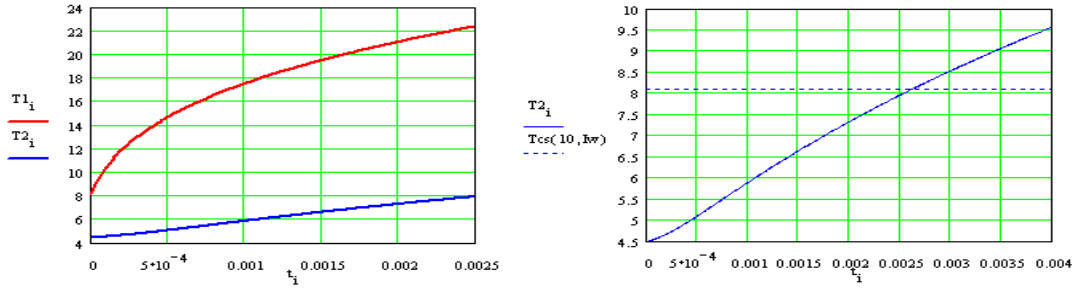

a) b)

Fig. 16: Temperature rise for the quench propagating radially: I = 300 A, n = 10

On the other hand, from the graph in Fig. 17 it is possible to see how the critical current for the layer # 10 changes in time due to increase of temperature. It reached the value I = 300 A at ~ 0.024 s, which is in a good agreement with Fig. 16b.

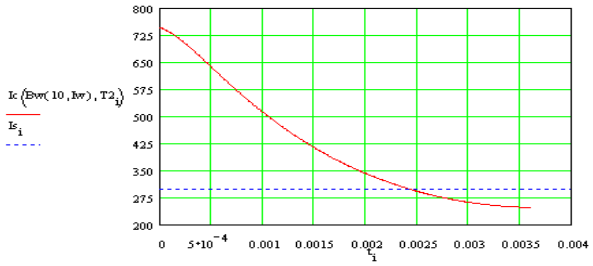

Fig. 17: Critical current change in time

Similar characteristics were taken for I ∈ (200A – 330A) and n ∈ (1 – 20) and for each case quench delay time was found. Graphs in Fig. 18 summarize the findings. Both graphs in Fig. 18 are identical, just scale was changed to "log" for the second graph to properly compare it with the graph shown in Fig. 15.

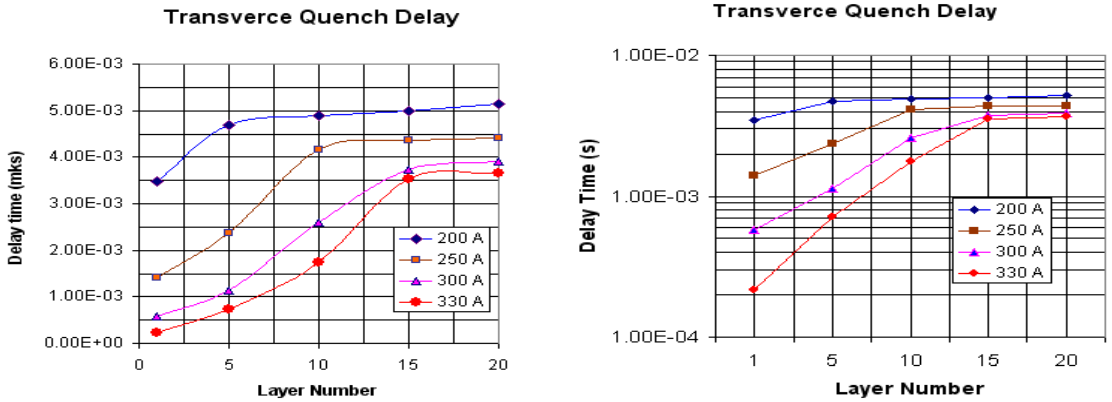

Fig. 18: Quench propagation delay in the radial direction

III-3. Axial Quench Propagation

Similar work was done to study propagation is the axial direction. In this case, for each layer of the coil, delay time stays constant because of our assumption that magnetic field does not change along the layers (long solenoid assumption). Curves in Fig. 19 summarize the results.

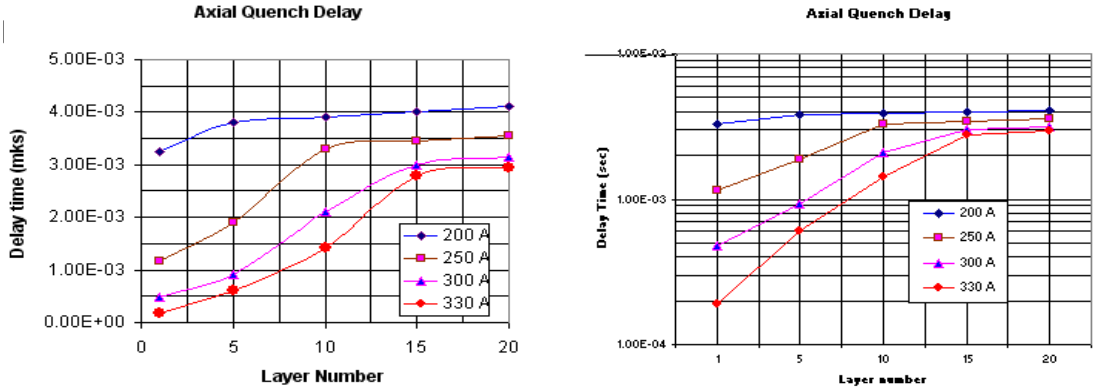

Fig. 19: Quench propagation delay in radial direction

Comparing Fig. 18 and Fig. 19, it is easy to notice that the values of the delays in the axial and radial directions are quite close. This is the result of quite compact winding with thin insulation between the layers and turns. To simplify further work, we will accept identical propagation properties in both directions. Comparison with propagation along the strand (Fig. 15) shows that the quench front propagation along the strand happens significantly (~ 5 times) slower. This means that the transverse axial quench propagation will rule movement of the quench boundary in the body of the coil.

To complete this part of the study, it is necessary to come out with an expression for the turn-to-turn propagation delay time. Based on what was shown in Fig. 18 and Fig. 19, relatively simple form was found to provide a satisfactory description of the effect. The expression is provided below and corresponding graph is shown in Fig. 20, which can be compared with the graphs in Fig. 18 and 19.

$$T(n, I) = 2.3\cdot10^{-4}\cdot[n+9.57\cdot10^{-3}\cdot(330 - I)^{1.5}] \quad \text{if} \quad n < 17 - 6\cdot10^{-4}\cdot(330 - I)^2$$

$$T(n. I) = 2.3\cdot10^{-4}\cdot[17 - 6\cdot10^{-4}\cdot(330 - I)^2 + 9.57\cdot10^{-3}\cdot(330 - I)^{1.5}] \quad \text{otherwise}$$

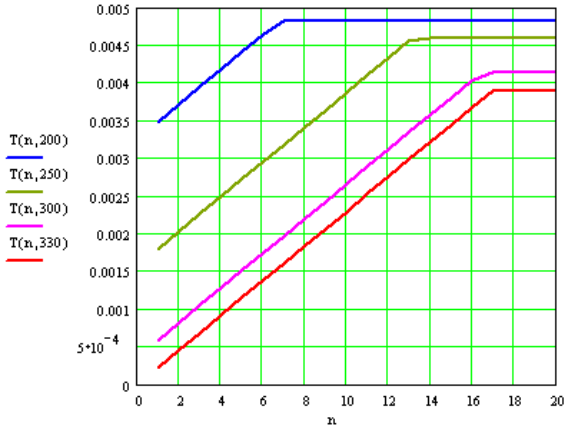

Fig. 20: Quench propagation delay in the transverse direction.

III-4 Quench propagation status

Now we can put together a picture of how quench would propagate in the coil after it started in the middle of the central turn of the first layer. As we have found earlier, quench propagation along the strand, although having higher velocity, can not compete with the transverse propagation, but can help equalizing delay times of radial and axial quench propagation. As it is possible to see from Fig. 20, delay time increases with the layer number. For this reason, the fastest way quench propagates to the particular turn (**m, n**) within the coil is that it travels first in the first layer to the axial position of the turn "**m**" and then in the radial direction to the layer "**n**" the turn is in. So, at given current, quench delay time to any turn in the body of the coil can be described by the next expression:

$$Del(m,n,I) := (m-1)\cdot Delay(1,I) + \sum_{k=1}^{n-1} Delay(k,I)$$

Knowing when a particular turn quenches allows visualizing quench propagation to different currents and in time. A series of charts in Fig. 21 present the status charts for the three sets of currents: 330 A, 250 A and 200A.

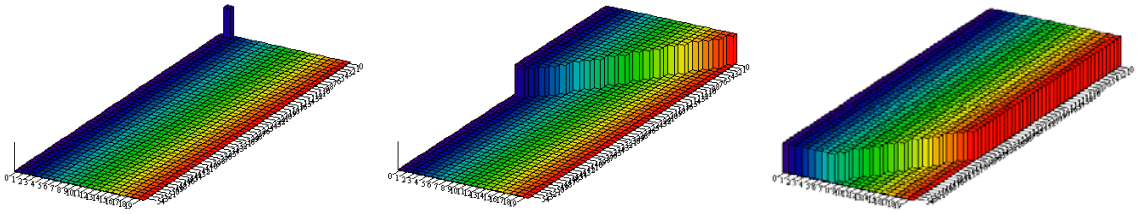

a) I = 200 A; t = 3.5 ms, 90 ms, 220 ms

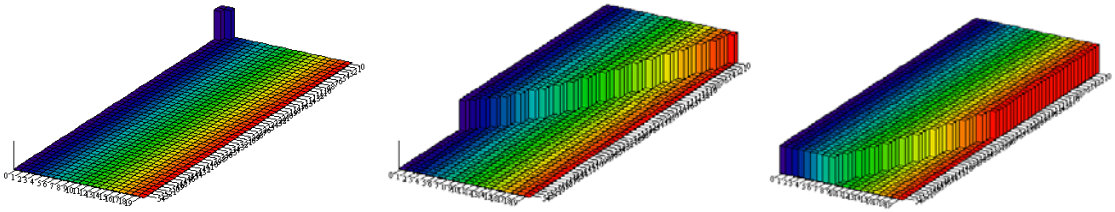

b) I = 250 A, t = 2 ms, 70 ms, 120 ms

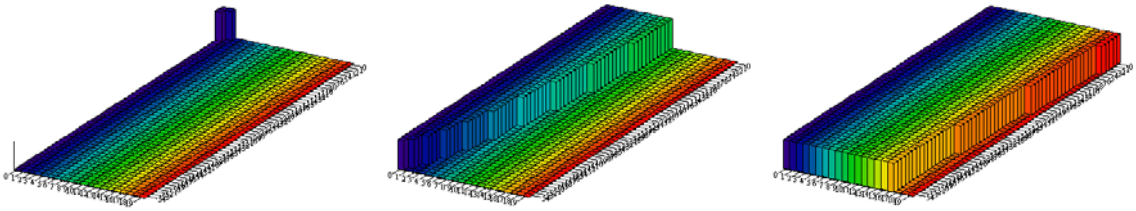

c) I = 330 A, t = 0.3 ms, 12.5 ms, 44 ms

Fig. 21: Quench propagation status

If coil current is 200 A, quench propagation speed almost does not depend on the direction of propagation. The reason is that at this current critical temperature is close to its ultimate value of 9.2 K, so it does not change much from layer to layer. In this case, the quench front reaches the outmost layer in ~ 90 ms and all the turns in the coil are normal in about 250 ms. With the 250 A, the quench propagates faster in the axial direction. It reaches the outer layer in ~ 70 ms, and all the turns turn become normal in about 140 ms. At 330 A, which is close to the ultimate current of the solenoid, quench front is almost parallel to the axis. This is due to fast propagation in the first layer, which becomes normal in ~ 12 ms. In about 50 ms all the coil becomes normal conducting.

IV. Coil Heating and Current Decay

Knowing when a particular turn quenches helps to solve the heating problem. In the adiabatic case, as we know when the heating starts for each turn, we can find what the temperature is at this location. This can be done by using a relationship representing an energy balance case:

$$\int_0^t I^2(t)dt = A_{tot}^2 \int_{T_b}^{T} \frac{C_p(T)}{\rho(T,B)} dT$$

The integral on the left side is usually referred to as ***IIt***. We will consider in this study that the onset of a quench is detected instantly, and at the same moment the power supply is insulated from the coil and the coil's leads are shorted. In this case the current shape during the quenching process will depend on how the temperature profile in the coil changes in time. **Before we know this profile, we will accept that I = const. Corresponding correction will be made later based on the obtained temperature profile during the first iteration.**

For the specific resistance and thermal capacity in the right hand integral above, we must use data averaged through the cross-section of the strand and the coil, taking into the account compaction factor and copper-to-non-copper ratio.

As it is clear from Fig. 7, the impact of magnetic field on the copper specific resistance is only significant in the beginning of the quenching process, when the temperature is low. This specific resistance does not change much in the range of fields between 1T and 8 T. So, not making a significant mistake, while evaluating specific resistance, we will use data for B = 7 T. Fig. 22 shows ***IIt*** dependence on the temperature, which is a parameter for the integral on the right side of the expression above. It means that to obtain certain temperature, corresponding value of ***IIt***-s must be reached. Reversing this graph, we get strand temperature as a function of IIt-s.

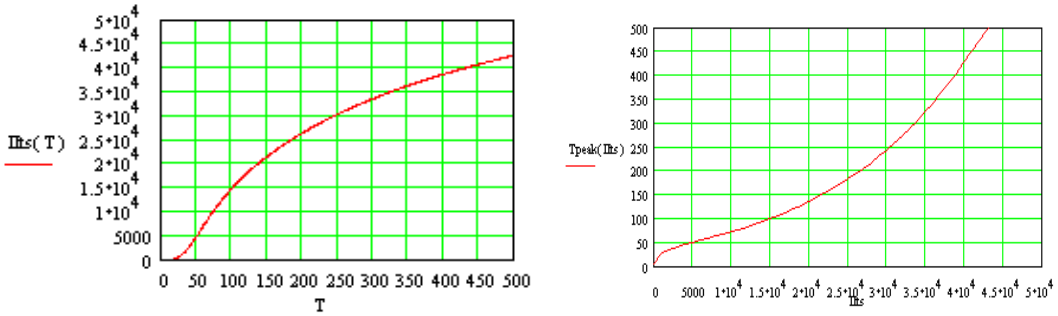

Fig. 22: Temperature of a turn as a function of the acting IIT-s

This type of temperature dependence on *IIt* is quite typical and can be found in many text books. If we can find *IIt* for any turn, we can calculate its temperature. It is possible to do so because we know when each turn becomes normal conducting:

$$IIT(m,n,I,t) := if\left[t - Del(m,n,I) > 0, I^2 \cdot (t - Del(m,n,I)), 0\right]$$

Fig. 23 visualizes some results of this evaluation for I = 300 A for different turn positions "m, n". Because I = const at this point, all the lines are straight and start at different times because of different delays.

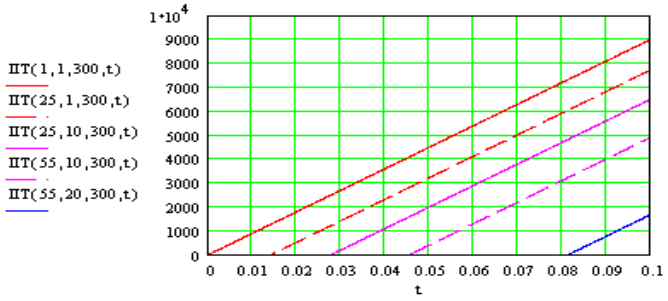

Fig. 23: IIt's of the coil's turns as a function of time

Knowing *IIt*-s and how the turn temperature depends on *IIt*-s, we can plot the temperature of every turn against time, as it is shown in Fig. 24 below.

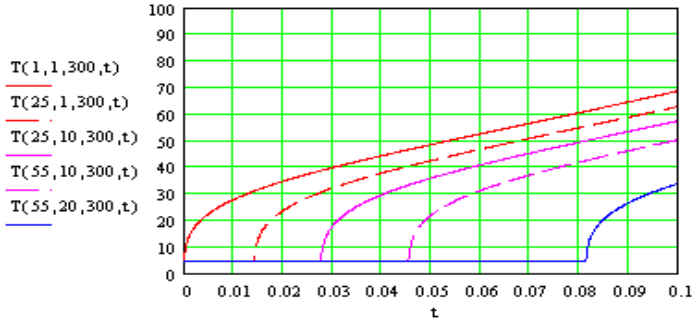

Fig. 24: Temperature of the coil's turns as function of time

It is possible to see that, as one could expect, the hottest spot is in the middle of the first layer. We need to remember that at this stage we have constant current in the coil. That's why temperature continues growing linearly. This result must be corrected after we find how the current decays with time. Hence, we need to know how the resistance of the coil changes with time. Turn resistance can be calculated using the next expression:

$$R(m,n,I,t) := \text{if}\left(t > \text{Del}(m,n,I), \frac{2\cdot\pi\cdot\text{rad}(n)}{\text{Atot}}\cdot\text{rhocomp}(T(m,n,I,t)), 0\right)$$

Corresponding graphs are shown in Fig. 25 below.

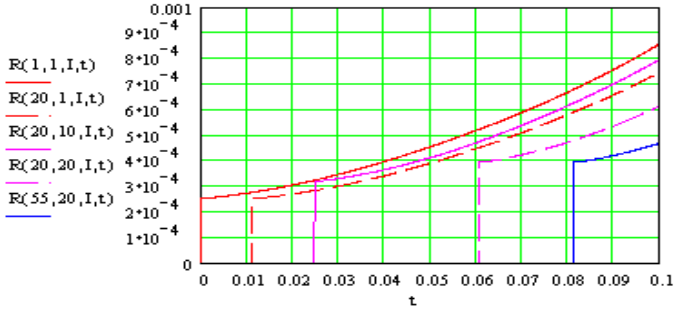

Fig. 25: Resistance of turns in the coil vs time.

Taking a sum of turn resistances, layer resistance can be found. This appeared to be quite time consuming in the MathCad environment. Parameterization of layer resistances was used to save computing time for the expense of loosing some accuracy though. The series of graphs in Fig. 26 compares layer resistances found by "honest" computation (on the left side) with what the parameterization gives.

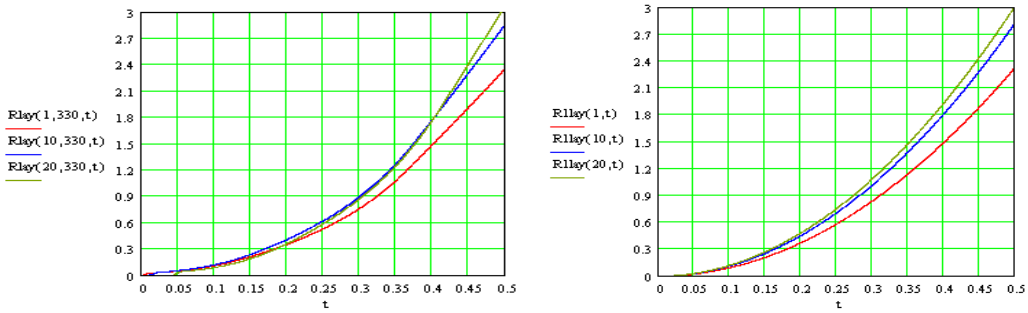

Fig. 26-a: Layer resistance. I = 330 A; $R1lay(n,t) = 12\cdot t^2\cdot[1 - 6.3\cdot10^{-4}\cdot(20 - n)^2]$

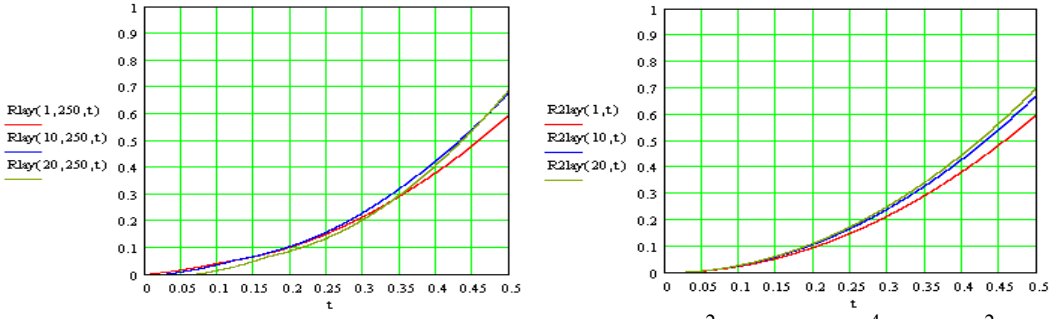

Fig. 26-b: Layer resistance. I = 250 A; $R2lay(n,t) = 2.8 \cdot t^2 \cdot [1 - 4.0 \cdot 10^{-4} \cdot (20 - n)^2]$

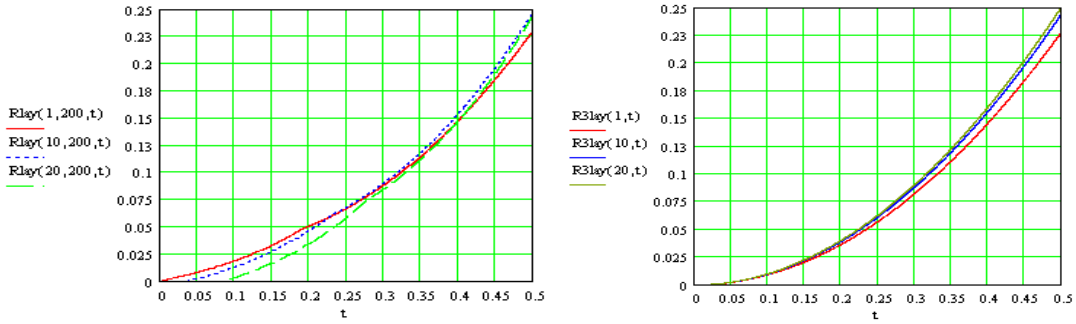

Fig. 26-c: Layer resistance. I = 2o0 A; $R2lay(n,t) = 1.0 \cdot t^2 \cdot [1 - 2.5 \cdot 10^{-4} \cdot (20 - n)^2]$

We will need data for layer resistance when voltage to ground is calculated as it will become clear later.

The total resistance of the coil is found by the taking a sum of resistances of all the layers. Graph in Fig. 27 compares "honestly" computed resistance of the coil (on the left side) with the suggested parametric expression that will be used in further studies:

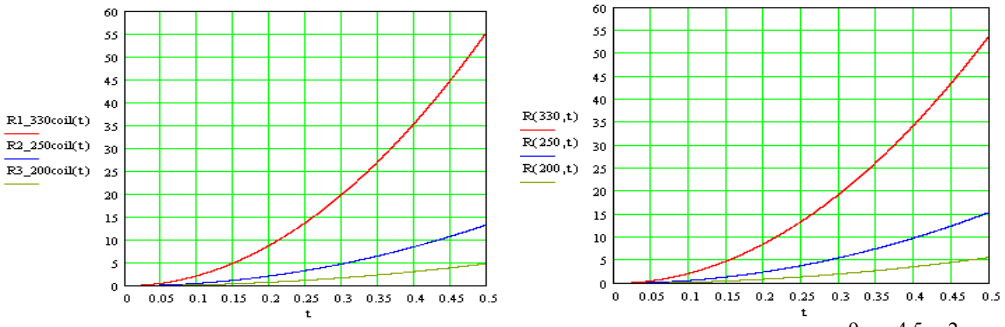

$$R(I_0, t) = 1.0 * 10^{-9} * I_0^{4.5} * t^2$$

Fig. 27: Coil resistance

As we saw earlier, at 200 A coil is fully normal at the moment t = 0.25 s. This means that the quadratic law one sees in the graphs is not due to quench propagation, but rather due to copper specific resistance dependence on temperature. This quadratic law only takes place when the coil current is constant, which can happen if the power supply is on after quench. The power supply can support this current only if the voltage drop across the coil does not exceed nominal voltage of the power supply. In reality, with 10 kW power supply (30 V at 330 A), the resources of the power source will expire at the moment $t \approx 20$ ms. This means that the graphs in Fig. 27 can not represent real dynamics of the resistance change in the coil beyond this time mark.

As was agreed before, we consider the coil separated from the power source immediately after quench detection and the two leads of the coil connected. Then the current in the coil can be defined using the next expression:

$$I_c(t, I_0) = I_0 \cdot \exp\left(-\int_0^t \frac{R(I_0, x)}{L_c} dx\right)$$

The inductance of the coil can be easily calculated as we know all geometrical and winding parameters of the coil: $L_c = 0.16$ H. Fig. 28 presents corresponding current decay graphs (on the left side) and compares them with what an appropriately chosen analytical expression gives:

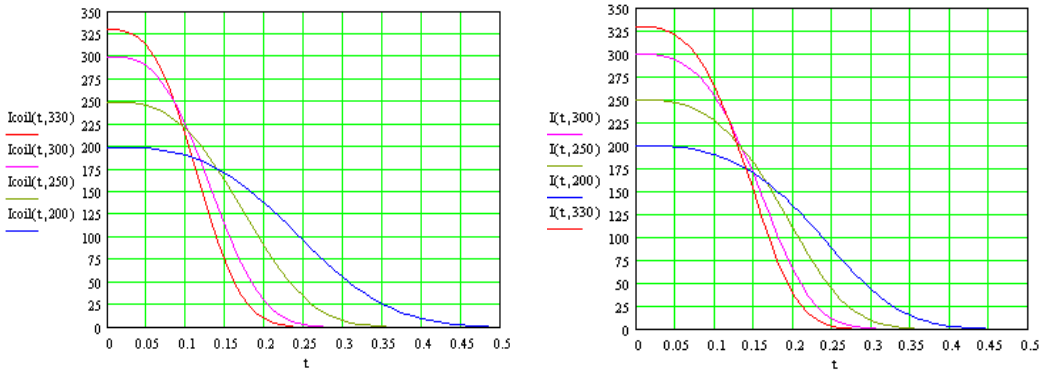

$$I(t, I_0) = \frac{2 \cdot I_0}{1 + \exp\left[\left(\frac{t \cdot I_0}{46}\right)^{2.8}\right]}$$

Fig. 28: Coil current: the first iteration

Because coil resistance that we used till this moment is clearly much higher than what can be in reality, when the current decays with time. As a result we should expect that it is going to take longer time for the current to decay. For how much longer will become clear after we recalculate coil resistance dynamics using the new current shape. This is done in the companion note TD-06-004.

References:

1. M. Wilson. Superconducting Magnets. Clarendon Press, Oxford, 1983.